CHAPTER 96

WAVE FORCE ON A VESSEL TIED AT OFFSHORE DOLPHINS

Yoshimi Goda
and
Tomotsuka Yoshimura

Marine Hydrodynamics Division, Port and Harbour Research Institute, Ministry of Transport, Nagase, Japan

ABSTRACT

The solution of wave scattering by a vertical elliptical cylinder is applied to calculate the wave forces exerted upon it. The wave forces in the directions of long and short axes of ellipsis are shown in nondimensional forms as the functions of the angle of wave approach, the diameter-to-wavelength ratio, and the aspect ratio of ellipsis. The results of wave force computed are also shown in terms of the virtual mass coefficients associated with the reference volume of the circular cylinder the diameter of which is approximately equal to the apparent width of the elliptical cylinder observed from the direction of wave approach.

Theory is further applied for the wave forces acting upon a vessel moored tight at offshore dolphins and the forces transmitted to the dolphins through the vessel. The vessel is approximated with the fixed elliptical cylinder having the same width-to-length ratio. The computation with directional wave spectra shows that a tanker of 200,000 D.W.T. may exert the force of about 1,400 tons at the one-third maximum amplitude to each breasting dolphin when the tanker is exposed to the incident waves of $H_{1/3}$=1.0m and $T_{1/3}$=10 sec from the broadside.

INTRODUCTION

Modern tankers and ore carriers are in a steady increase in their size in order to lower the transportation cost of their cargo. A number of berthy facilities for them have recently been constructed in the offshore. The berthing facilities are called sea berths.

Engineers examine the conditions of winds, waves, tidal currents, tides, soils, and earthquakes in the design of a sea berth, but the major design load usually comes from the impact of ship's berthing or the earthquake force. The wave forces acting upon breasting dolphins through the vessel moored are not taken into design in spite of their apprehended importance, because their magnitude has yet been uncertain.

When a tanker with the length of 300 to 400 m is moored at a sea berth, it behaves like a kind of an insular breakwater and is expected to receive large wave forces. The forces must be transmitted to the dolphins. Thus, the wave forces can be one of major design factors for offshore dolphins.

The authors have previously derived the solution of wave scattering by a vertical, elliptical cylinder, and have confirmed its validity for the case of insular breakwaters through several experiments.[1] The solution is extended in this paper to yield the wave forces exerted upon an elliptical cylinder. The solution is applied for wave forces upon a vessel, the geometry of which is approximated with the elliptical cylinder having the same aspect ratio. The vessel is also assumed to be tightly fixed at two breasting dolphins. Computation of wave forces are made for incident waves having directional spectrum. The computed irregular forces are shown with the one-third maximum value as the representative of the force spectra.

SOLUTION OF SCATTERED WAVES BY AN ELLIPTICAL CYLINDER

The potential theory is presumed in order to solve the scattering of small amplitude waves. From the presumption, the fluid motion and boundary conditions are expressed as

$$\frac{\partial^2 \Phi}{\partial x^2} + \frac{\partial^2 \Phi}{\partial y^2} + \frac{\partial^2 \Phi}{\partial z^2} = 0 \qquad \text{(in fluid)} \qquad (1)$$

$$\left.\begin{aligned} \frac{\partial \zeta}{\partial t} &= \left(\frac{\partial \Phi}{\partial Z}\right)_{z=0} && (2) \\ \zeta &= -\frac{1}{g}\left(\frac{\partial \Phi}{\partial t}\right)_{z=0} && (3) \end{aligned}\right\} \quad \text{(on water surface)}$$

$$\frac{\partial \Phi}{\partial n} = 0 \qquad \text{(on the obstacle surface and the sea bottom)} \qquad (4)$$

where x and y are the coordinates on the still water surface, z is the coordinate measured from water surface positive upward, ζ is the water surface displacement, g is the acciration of gravity, and n is the coordinate normal to the boundary surface.

The velocity potential Φ which satisfies the boundary condition at the sea bottom is expressed as

$$\Phi = \phi_0 \phi \cosh k(h+z) \exp(i\sigma t) \qquad (5)$$

where ϕ_0 is a constant, ϕ is a function describing the profile of water surface, $k=2\pi/L$, $\sigma=2\pi/T$, L is the wavelength, T is the wave period, and h is the water depth.

The relation among wave period, wave length and water depth is derived from Eq. (2), (3) and (5) as

$$\sigma^2 = g\ k\ \tanh kh \tag{6}$$

By the substitution of Eq. (5) into Eq. (1)

$$\frac{\partial^2 \phi}{\partial x^2} + \frac{\partial^2 \phi}{\partial y^2} + k^2 \phi = 0 \tag{7}$$

In the case that the boundary is represented with a vertical elliptical cylinder the problem is better treated by transfering the coordinates (x, y) with the elliptical coordinates (ξ , η) shown by Fig. 1 as

$$\left.\begin{aligned} x &= \frac{B}{2} \cosh \xi \quad \cos \eta \\ y &= \frac{B}{2} \sinh \xi \quad \sin \eta \end{aligned}\right\} \tag{8}$$

where B is the distance between the focuses of the ellipsis. By using Eq. (8) Eq. (7) is transformed as

$$\frac{8}{B^2(\cosh 2\xi - \cos 2\eta)} \left(\frac{\partial^2 \phi}{\partial \xi^2} + \frac{\partial^2 \phi}{\partial \eta^2}\right) + k^2 \phi = 0 \tag{9}$$

The water surface function $\emptyset$ can be expressed with the addition of $\emptyset_{in}$ of the incoming waves and $\emptyset_{sc}$ of the scattered waves by the principle of linearity. Since $\lim_{\xi \to \infty} \emptyset_{sc} = 0$, both $\emptyset_{in}$ and $\emptyset_{sc}$ must be the solution of Eq. (9).

Presuming that $\emptyset$ is expressed as the product of the function R(ξ) of only ξ and Q(η) of only η , Eq. (9) is

$$\frac{d^2R}{R\, d\xi^2} + 2\, k_1^2 \cosh 2\xi = -\frac{d^2Q}{Q\, d\eta^2} + 2\, k_1^2 \cos 2\eta = A \tag{10}$$

In Eq. (10) A is the characteristic number which is determined with only k_1^2 , where $k_1 = B\, k/ 4 = \pi B / 2 L$.

Equation (10) can be separated into two equations for R(ξ) and Q(η).

$$\frac{d^2Q}{d\eta^2} + (A - 2\, k_1^2 \cos 2\eta)\, Q = 0 \tag{11}$$

$$\frac{d^2R}{d\xi^2} - (A - 2\, k_1^2 \cosh 2\xi)\, R = 0 \tag{12}$$

When $\eta = \eta^* + n\pi$ is substituted into η in Eq. (11), the form of the equation does not change. Therefore, one of the solutions of Eq. (11) has a periodic function with the period of π or 2π . When $\eta = \xi / i$ is substituted into η in Eq. (11), Eq. (11) become the same equation with Eq. (12). Thus the solutions of either equations, (11) or (12), immediately yield the solutions of another. Equations (11) and (12) are the Mathieu differential equation and the moditied Mathieu differential equation.[2)]

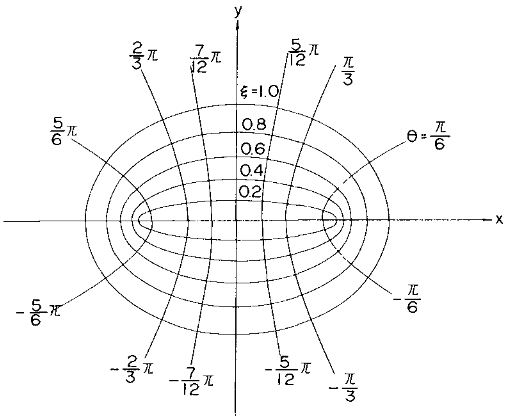

Fig. 1 Elliptical coordinates

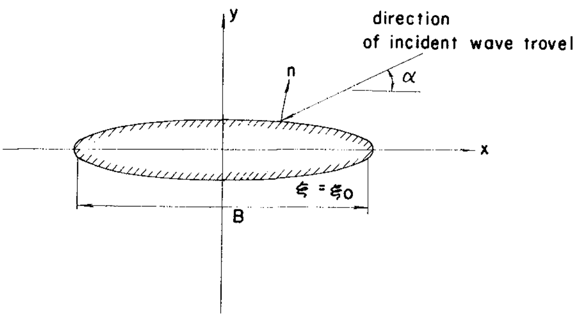

Fig. 2 Elliptical cylinder and direction of incident wave travel

When the incident waves approach the elliptical cylinder from the direction shown in Fig. 2, the waves are expressed as the series of the solutions of Eq. (11) and (12).

$$\phi_{in} = \sum_{n=0}^{\infty} \left[\frac{2}{p_{2n}} Ce_{2n}(\xi)\, ce_{2n}(\eta)\, ce_{2n}(\alpha) \right.$$

$$+ \frac{2}{s_{2n+2}} Se_{2n+2}(\xi)\, se_{2n+2}(\eta)\, se_{2n+2}(\alpha)$$

$$+ i \left\{ \frac{2}{p_{2n+1}} Ce_{2n+1}(\xi)\, ce_{2n+1}(\eta)\, ce_{2n+1}(\alpha) \right.$$

$$\left.\left. + \frac{2}{s_{2n+1}} Se_{2n+1}(\xi)\, se_{2n+1}(\eta)\, se_{2n+1}(\alpha) \right\} \right] \tag{13}$$

The functions $ce_n(\eta)$ and $se_n(\eta)$ are the solutions of Eq. (11); the former is the even function and the latter the odd. The functions $Ce_n(\xi)$ and $Se_n(\eta)$ are the solutions of Eq. (12) and correspond to $ce_n(\eta)$ and $se_n(\eta)$ respectively. The terms p_n and s_n are constants.

Considering that the scattered waves progress outward from the cylinder, ϕ_{sc} can be expressed as

$$\phi_{sc} = \sum_{n=0}^{\infty} C_{2n}\, Me^{(2)}_{2n}(\xi)\, ce_{2n}(\eta)\, ce_{2n}(\alpha)$$

$$+ S_{2n+2}\, Ne^{(2)}_{2n+2}(\xi)\, se_{2n+2}(\eta)\, se_{2n+2}(\alpha)$$

$$+ C_{2n+1}\, Me^{(2)}_{2n+1}(\xi)\, ce_{2n+1}(\eta)\, ce_{2n+1}(\alpha)$$

$$+ S_{2n+1}\, Ne^{(2)}_{2n+1}(\xi)\, se_{2n+1}(\eta)\, se_{2n+1}(\alpha) \tag{14}$$

The functions $Me^{(2)}_n(\xi)$ and $Ne^{(2)}_n(\xi)$ in Eq. (14) are the another solutions of Eq. (12) and correspond to the second kind of the Hankel function. The constants C_n and S_n are determined by the boundary condition on the elliptical cylinder of the following.

$$\left(\frac{\partial \phi_{in}}{\partial \xi}\right)_{\xi=\xi_0} + \left(\frac{\partial \phi_{sc}}{\partial \xi}\right)_{\xi=\xi_0} = 0 \tag{15}$$

The water surface function ϕ is thus obtained from Eq. (13), (14) and (15).

$$\begin{aligned}\phi &= \phi_{in} + \phi_{sc} \\ &= \sum_{n=0}^{\infty}\Bigg[\frac{2}{p_{2n}}\left(Ce_{2n}(\xi) - \frac{Ce'_{2n}(\xi_0)}{Me^{(2)'}_{2n}(\xi_0)} Me^{(2)}_{2n}(\xi)\right) ce_{2n}(\eta) ce_{2n}(\alpha) \\ &+ \frac{2}{s_{2n+2}}\left(Se_{2n+2}(\xi) - \frac{Se'_{2n+2}(\xi_0)}{Ne^{(2)'}_{2n+2}(\xi_0)} Ne^{(2)}_{2n+2}(\xi)\right) se_{2n+2}(\eta)\, se_{2n+2}(\alpha) \\ &+ i\Bigg\{\frac{2}{p_{2n+1}}\left(Ce_{2n+1}(\xi) - \frac{Ce'_{2n+1}(\xi_0)}{Me^{(2)'}_{2n+1}(\xi_0)} Me^{(2)}_{2n+1}(\xi)\right) ce_{2n+1}(\eta) ce_{2n+1}(\alpha) \\ &+ \frac{2}{s_{2n+1}}\left(Se_{2n+1}(\xi) - \frac{Se'_{2n+1}(\xi_0)}{Ne^{(2)'}_{2n+1}(\xi_0)} Ne^{(2)}_{2n+1}(\xi)\right) se_{2n+1}(\eta) se_{2n+1}(\alpha)\Bigg\}\Bigg]\end{aligned} \tag{16}$$

When the incoming wave height is H_{in}, ϕ_0 can be obtained from Eq. (3) as

$$\phi_0 = \frac{gH_{in}}{2\sigma \cosh kh} \tag{17}$$

The velocity potential of Φ becomes

$$\Phi = \frac{gH_{in}}{2\sigma}\, \phi\, \frac{\cosh k(h+z)}{\cosh kh} \exp(i\sigma t) \tag{18}$$

Before the calculation of the wave form and forces by the velocity potential of Eq. (18), the characteristic number and other constants must be computed. The number of terms in the summations is determined from the convergency of the series of Eq. (16). The number generally becomes large as B/L increases. In the present paper the number is determined with sufficient accuracy as shown in Table 1.

Table 1. Number of Terms

B/L	≦1.2	≦2.4	≦3.2	≦4.5	≦5.5	≦6.5	≦7.5	≦8.0
Number of Terms	1～2	1～3	1～4	1～5	1～6	1～7	1～8	1～9

THE WAVE FORCES ACTING UPON THE ELLIPTICAL CYLINDER

The formula of the wave pressure at the point (ξ_0, η, z) on the cylinder surface is derived from the velocity potential of Eq. (18) by the use of the Bernoulli equation as

$$p = -i\frac{w_0 H_{in}}{2}\frac{\cosh k(h+z)}{\cosh kh}(\phi)_{\xi=\xi_0} \tag{19}$$

in which w_0 is the specific weight of water. The functions $ce_n(\eta)$ and $se_n(\eta)$ in $(\phi)_{\xi=\xi_0}$ are rewritten with the Fourier series of η for the sake of fast convergence as:

$$\begin{aligned}
ce_{2n}(\eta) &= \sum_{r=0}^{\infty} A_{2r}^{(2n)} \cos 2r\eta \\
ce_{2n+1}(\eta) &= \sum_{r=0}^{\infty} A_{2r+1}^{(2n+1)} \cos(2r+1)\eta \\
se_{2n+1}(\eta) &= \sum_{r=0}^{\infty} B_{2r+1}^{(2n+1)} \sin(2r+1)\eta \\
se_{2n+2}(\eta) &= \sum_{r=0}^{\infty} B_{2r+2}^{(2n+2)} \sin(2r+2)\eta
\end{aligned} \tag{20}$$

The terms $A_r^{(n)}$ and $B_r^{(n)}$ are functions of k_1^2.

The total wave forces exerted upon the cylinder are obtained by the double integrations of wave pressure from the bottom to the still water level and around the cylinder. The total forces are separated into the component forces Fx and Fy in the x- and y-directions. The results of calculations are:

$$\left.\begin{aligned}
Fx &= \frac{\pi w_0 bH_{in}}{4k}\tanh kh \exp(i\sigma t) \\
&\times \sum_{n=0}^{\infty} \frac{2A_1^{(2n+1)}}{p_{2n+1}}\left\{Ce_{2n+1}(\xi_0) - \frac{Ce'_{2n+1}(\xi_0)}{Me_{2n+1}^{(2)'}(\xi_0)} Me_{2n+1}^{(2)}(\xi_0)\right\} ce_{2n+1}(\alpha) \\
Fy &= -\frac{\pi w_0 aH_{in}}{4k}\tanh kh \exp(i\sigma t) \\
&\times \sum_{n=0}^{\infty} \frac{2B_1^{(2n+1)}}{s_{2n+1}}\left\{Se_{2n+1}(\xi_0) - \frac{Se'_{2n+1}(\xi_0)}{Ne_{2n+1}^{(2)'}(\xi_0)} Ne_{2n+1}^{(2)}(\xi_0)\right\} se_{2n+1}(\alpha)
\end{aligned}\right\} \tag{21}$$

where a and b are the long and short axes of ellipsis, respectively.

Figures 3 and 4 show the variation of the nondimensional forms of Fx and Fy with respect to the ratio a/L in the case of b/a = 0.15. The nondimensional forces are $Fx/w_oH_{in}\ b\ h\ K_F$ and $Fy/w_oH_{in}\ a\ h\ K_F$, where K_F is the coefficient derived from the wave pressure of a small amplitude wave:

$$K_F = \frac{\tanh kh}{k\ h} \tag{22}$$

The nondimensional forces exhibit undulations, but the periods and amplitudes of undulations vary according to the angle α of the incident wave approach and the ratio of a/L. The nondimensional force in the y-direction has the maximum value at about a/L = 0.4 in every value of α, and decreases rapidly in the range of $a/L > 1.0$ except for $\alpha = 90^o$. The undulation of Fx in nondimensional form is larger than that of Fy, but the maximum value of Fx is almost constant regardless of the incident angle α. The heavy lines in Figs. 3 and 4 indicate the nondimensional forces upon a circular cylinder.

VIRTUAL MASS COEFFICIENTS OF THE ELLIPTICAL CYLINDER

The amplitude of wave forces of Fx and Fy can be expressed in terms of the virtual mass coefficient associated with the accelation of water particles under progressive waves. Since the virtual mass coefficient depends on the parameters of a/L, α, and b/a, the variation of its value is much complicated. To simplify the computation the reference volume of a circular cylinder is applied. The diameter of the circular cylinder is taken approximately equal to the apparent width of the elliptical cylinder observed from the direction of the incident wave approach. The diameter of D is expressed as

$$D = (a - b) \sin\alpha + b \tag{23}$$

The diameter D in Eq. (23) satisfies the definition of apparent width at certain conditions of α, a, and b as follows

$$\left.\begin{array}{llll} D = b & \text{at} & \alpha = 0 & \\ D = a & \text{at} & \alpha = \pi/2 & \\ D = a = b & \text{at} & a = b & \text{(circular cylinder)} \\ D = a \sin\alpha & \text{at} & b = 0 & \text{(plate)} \end{array}\right\} \tag{24}$$

The virtual mass coefficients of Cmx and Cmy can be computed from Eq. (25)

$$\left.\begin{aligned} Fx &= \frac{w_o}{g}\, Cmx\, \frac{\pi}{4} D^2 \int_{-h}^{o} \frac{\partial u}{\partial t}\, dz \\ Fy &= \frac{w_o}{g}\, Cmy\, \frac{\pi}{4} D^2 \int_{-h}^{o} \frac{\partial v}{\partial t}\, dz \end{aligned}\right\} \tag{25}$$

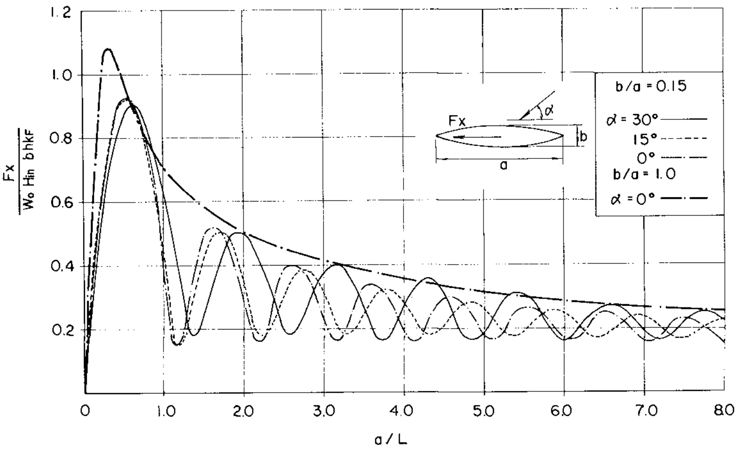

Fig. 3 Variation of nondimensionarized force of Fx

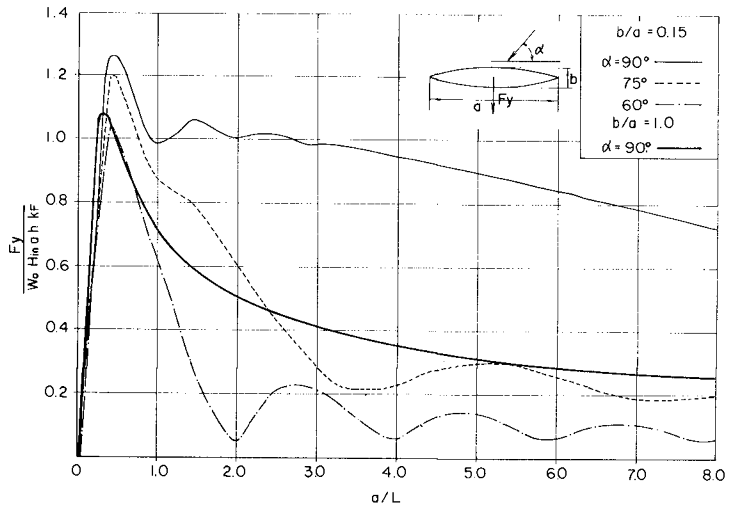

Fig. 4 Variation of nondimensionarized force of Fy

The symbols u and v in Eq.(25) denote the water particle velocity in x- and y-direction under progressive waves without the obstacle. Figures 5 and 6 show examples of the variations of Cmx and Cmy with respect to D/L for $\alpha = 90^{\circ}$ and 60°, respectively. There is no line of Cmx in Fig. 5 for $\alpha = 90^{\circ}$ because of Fx = 0 at $\alpha = 90^{\circ}$.

The line of b/a = 0.0001 gives the asymptote to the virtual mass coefficient of a plate, and the line of b/a = 1.0 represents the virtual mass coefficient of a circular cylinder computed by the formula derived by MacCamy & Fuchs.[3] The coefficient Cmy for b/a = 0.0001 at D/L = 0 and $\alpha = 90^{\circ}$ has the value of 1.0, which is equal with the theoretical value of a plate.

Diagrams of Cmx and Cmy for other directions of wave approach can be found in reference (4).

IRREGULAR FORCES ACTINC ON A VESSEL AND OFFSHORE DOLPHINS

(1) Wave Spectrum

The relation between the frequency wave spectrum of $S_{\zeta\zeta}(f)$ and the directional wave spectrum $S_{\zeta\zeta}(f,\theta)$ is

$$S_{\zeta\zeta}(f) = \int_{-\pi}^{\pi} S_{\zeta\zeta}(f,\theta)\,d\theta \tag{26}$$

The directional wave spectrum $S_{\zeta\zeta}(f,\theta)$ is expressed as the product of frequency-wise function $S_{\zeta\zeta}(f)$ and directional function of $h(\theta)$ which satisfies the condition of

$$\int_{-\pi}^{\pi} h(\theta)\,d\theta = 1, \tag{27}$$

then $S_{\zeta\zeta}(f)$ coincides with the frequency wave spectrum. The functional forms of frequency wave spectra have been proposed by Neumann[5], Bretschneider[6], Pierson & Moskowitz[7], and etc. The forms of the angular distribution of $h(\theta)$ have been investigated in the wave measurements by Cote et. al.[8] and Ewing[9], but the functional form has not been settled on account of scanty measurements.

In this paper, the following Bretschneider's spectrum modified to satisfy the condition of $\overline{\zeta^2} = \int_0^{\infty} S_{\zeta\zeta}(f)\,df$ is used as the frequency wave spectrum.

$$S_{\zeta\zeta}(f) = 0.430\left(\frac{\bar{H}}{g\bar{T}}\right)^2 g^2 f^{-5} \exp\left[-0.645(\bar{T}f)^{-4}\right] \tag{28}$$

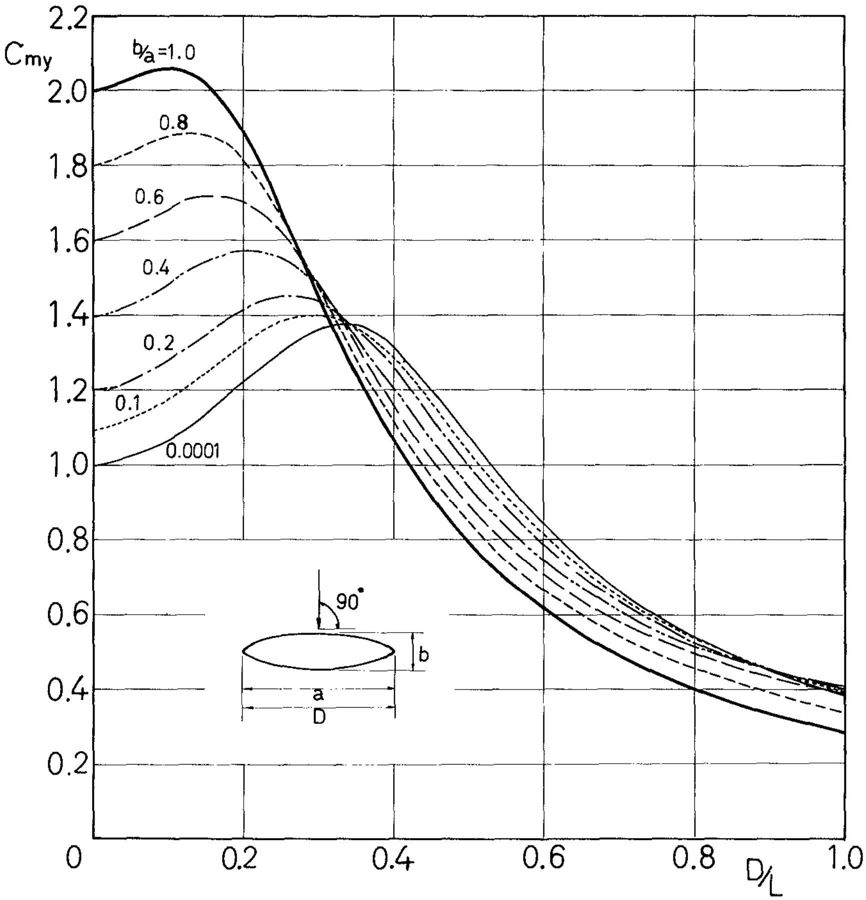

Fig. 5 Virtual mass coefficient Cmy

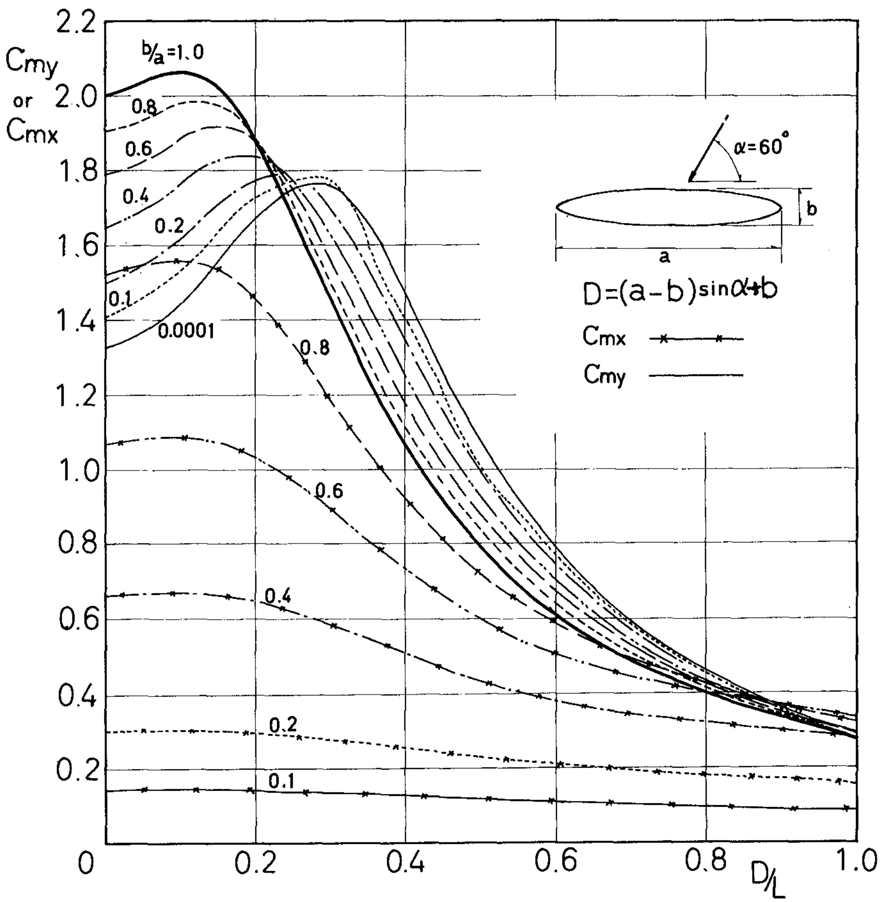

Fig. 6 Virtual mass coefficients Cmx and Cmy

As to the angular distribution satisfying Eq. (27), the following form is employed;

$$h(\theta)\begin{cases} = \dfrac{2^{2s}(s!)^2}{(2s)!\,\pi}\cos^{2s}\theta & (\theta = 1, 2, \cdots\cdots)\ (|\theta| < \frac{\pi}{2}) \\ = 0 & (|\theta| > \frac{\pi}{2}) \end{cases} \tag{29}$$

Computation of irregular wave forces is made with the relations of $\bar{H} = 0.625\,H_{1/3}$ and $\bar{T} = 0.9\,T_{1/3}$, where $\bar{H}$ and $\bar{T}$ are the mean wave height and period, and $H_{1/3}$ and $T_{1/3}$ are the wave height and period of the significant wave.

(2) Representative Value of the Irregular Forces

Because the wave forces are linear to the displacement of the water level as shown in Eq. (21) and the displacement almost has the Gaussian distribution, the irregular wave forces are expected to follow the same distribution. Longuet-Higgins has proved that the maxima of the wave configuration have the Rayleigh distribution in the case of the narrow-band spectra[10). Although the spectral band of the sea waves is wide, the investigations of sea waves by field measurements[11) and by numerical simulation[12) have demonstrated that the wave heights closely follow the Rayleigh distribution as long as they are defined by the zero-up-crossing method. Therefore, if the maxima of irregular wave forces are defined as the maximum between two successive zero-up-crossing points of a wave force record, the newly defined maxima will follow the Rayleigh distribution.

The one-third maximum force of $F_{1/3}$ and one-tenth maximum force of $F_{1/10}$ can be calculated under the Rayleigh distribution as

$$\begin{aligned} F_{1/3} &= 1.416\sqrt{\overline{F^2}} \fallingdotseq 2.00\sqrt{\int_0^\infty S_{FF}(f)\,df} \\ F_{1/3} &= 1.800\sqrt{\overline{F^2}} \fallingdotseq 2.55\sqrt{\int_0^\infty S_{FF}(f)\,df} \end{aligned} \tag{30}$$

The selection of which statistical values of $\sqrt{\overline{F^2}}$, $F_{1/3}$, or $F_{1/10}$ for the design of offshore structures cannot be easily determined without due consideration of the dynamic response or allowable strength of the material of the structures.

In this paper, $F_{1/3}$ is employed as the representative value of the irregular wave forces, and the results of the computations are expressed with it. It must be made clear that $F_{1/3}$ should not be taken as the design load because the force larger than $F_{1/3}$ is expected to occur during the given wave condition. If the design load is to be taken as the maximum force with the occurrance probability less than μ during the continuation of N waves, the maximum force can be calculated as:

$$(Fmax)_{\mu} = 0.708 F_{1/3} \sqrt{\ln\left(\frac{\ln N}{\ln 1/(1-\mu)}\right)} \tag{31}$$

With the occurrence probability selected at $\mu = 0.10$, $(Fmax)_{\mu}$ becomes 1.85 $F_{1/3}$ for 100 waves, and 2.14 $F_{1/3}$ for 1000 waves.

(3) Forces Acting upon the Vessel Tied at Offshore Dolphins

In the computation of wave forces acting upon a vessel moored tight at the offshore dolphins, the following four assumptions are introduced.

1) The geometry of the vessel is represented with a virtical, elliptical cylinder of Fig. 7 with the draft of h_1.
2) The vessel is considered to be rigidly tied at two breasting dolphins without movement though actual vessels in mooring have the freedom of limited motion. The wave forces computed under these assumptions will exceed those acting upon movable vessels and will provide the asymtotic values of thrusts and pulls.
3) The presence of the gap between the vessel's bilge and the sea bottom is assumed not to affect the pressure distribution along the vessel.
4) The wave force of Fx in the direction of the vessel length is taken by the tie ropes.

The two breasting dolphins are located at (x_R, y_R) and (x_L, y_L) shown in Fig. 7. In the formulation, the symbols in Fig. 7 is used.

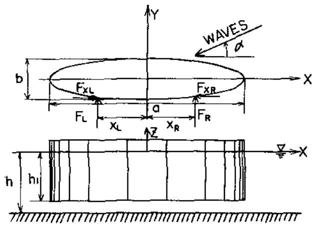

Fig. 7 Characteristics of computed tanker

Forces equilibrum equations are represented as

$$\left.\begin{aligned} & Fx_L - Fx_R = 0 \\ & F_L + F_R + Fy = 0 \\ & - F_L x_L - F_R x_R + M_o + Fx_L y_L - Fx_R y_R = 0 \end{aligned}\right\} \tag{32}$$

The forces Fx and Fy are the x and y component of the wave force acting upon the vessel, and can be computed under the previous assumptions. The symbols M_O denotes the moment by the wave force arround the origin. Fx_R and Fx_L are the forces generated by Fy for the existence of the curvature of the elliptical cylinder at the fixed points.

It is considered that $| y_R - y_L |$ is much shorter than x_L and x_R, and Fx_R and Fx_L are much smaller than Fy. When the terms containing Fx_R and Fx_L are neglected, F_L and F_R can be obtained from Eq. (32) as follows

$$\left.\begin{aligned} F_L &= -\frac{M_O + Fy\ x_R}{x_R - x_L} \\ F_R &= \frac{M_O + Fy\ x_L}{x_R - x_L} \end{aligned}\right\} \tag{33}$$

The value of Fx will determine the necessary strength of tie ropes and is obtained as

$$\begin{aligned} Fx &= \int_0^{2\pi}\int_{-h_1}^{0} \left(-\frac{B}{2}\sinh\xi_0\cos\eta\right) p\ dz\ d\eta \\ &= \frac{H_{in}}{2}\exp(i\sigma t)\sum_{n=0}^{\infty}(\Psi_{Fx})_n \end{aligned} \tag{34}$$

where,

$$(\Psi_{Fx})_n = -\frac{\pi w_0 b}{2k}\ \frac{\sinh kh - \sinh k(h-h_1)}{\cosh kh}$$

$$\times\left[\frac{2A_1^{(2n+1)}}{p_{2n}}\left\{Ce_{2n+1}(\xi_0) - \frac{Ce'_{2n+1}(\xi_0)}{Me^{(2)\prime}_{2n+1}(\xi_0)}\ Me^{(2)}_{2n+1}(\xi_0)\right\}ce_{2n+1}(\alpha)\right] \tag{35}$$

The force Fy can be easily obtained in the form similar with Eq. (35) in reference of Eq. (21). The moment M_O is

$$M_O = \int y\ dFx - \int x\ dFy \tag{36}$$

The forces of F_L and F_R is obtained by substituting Fx, Fy, and M_O into Eq. (33).

When $(\Psi_F)_n$ of each force is given in the same form with Eq. (35), the spectrum of each force of $S_{FF}(f)$ is calculated as:

$$S_{FF}(f) = \int_{-\pi}^{\pi} \left\{ \sum_{n,m=0}^{\infty} (\Psi_F)_n (\Psi_F)_m^* \right\} S_{\zeta\zeta}(f,\theta)\, d\theta$$

$$= S_{\zeta\zeta}(f) \int_{-\pi}^{\pi} \left\{ \sum_{n,m=0}^{\infty} (\Psi_F)_n (\Psi_F)_m^* \right\} h(\theta) d\theta \tag{37}$$

where $(\Psi_F)_n^*$ is the conjugate complex number of $(\Psi_F)_n$.

When the main directional angle of the irregular wave approach is θ_0 θ in Eq. (37) is given with $\theta = \alpha - \theta_0$.

The computations of the force spectra are made for a taker of 200,000 D.W.T. with the length of Ls = 352m, the width of Ws = 50.3m, and the draft of h_1 = 17.8m. The locations of the dolphins are assumed at x_R = 88m and x_L =-88m, which are a quarter of the length of the tanker.

Two types of the irregular incident waves are used in the computations. One is the swell of $H_{1/3}$ = 1.0m and $T_{1/3}$ = 10 sec. The other is the waves with a long period of $H_{1/3}$ = 0.2m and $T_{1/3}$ = 30 sec which are considered to exert a very strong force to the tanker. The water depth is constant as h = 20m.

Figure 8 shows the variation of the one-third maximum force of each irregular force to θ_0 in the case of $H_{1/3}$ = 1.0m and $T_{1/3}$ = 10 sec and the parameter of s = 1 in Eq. (29).

Each one-third maximum force is maximum at θ_0 = 90°. The one-third maximum forces of Fy, F_L and F_R decrease rapidly as θ_0 decrease, but the decrease of $Fx_{1/3}$ is very small as $Fx_{1/3}$ = 300 tons at θ_0 = 90° and 200 tons at θ_0 = 0°. In spite of the small height of significant waves, $H_{1/3}$ = 1.0m, the one-third maximum force of Fy acting upon the tanker is 1,950 tons at θ_0 = 90°, and both $F_{L1/3}$ and $F_{R1/3}$ acting upon the dolphins are 1,400 tons at the same angle.

Figures 9 and 10 show the variation of $Fy_{1/3}$ and $F_{R1/3}$ to the parameter of s in the case same with Fig. 8. The force $Fy_{1/3}$ is maximum at θ_0 = 90° and its value depends on the parameter s. For example, $Fy_{1/3}$ is 4,200 tons with s = ∞ , 2,500 tons with s = 4 and 1,950 tons with s = 1 at θ_0 = 90°. But $Fy_{1/3}$ with s = ∞ decreases most rapidly as θ_0 decreases from 90°. The variation of $F_{R1/3}$ has almost same tendency with that of $Fy_{1/3}$ except that $F_{R1/3}$ is maximum at about θ_0 = 80° with s = ∞ .

Figure 11 shows the variation of each one-third maximum force in the case of $H_{1/3}$ = 0.2m, $T_{1/3}$ = 30 sec and s = 1. Though the incident wave height is one-fifth of the previous cases, $Fy_{1/3}$ of 910 tons and $F_{L1/3}$ = $F_{R1/3}$ of 590 tons are about one halves of those in Fig. 8. These forces decrease rapidly with the decrease of θ_0, but $Fx_{1/3}$ is almost constant.

When it is considered that even incident waves of a small wave height can exert very large forces to the tanker and the offshore dolphins as mentioned above, the wave forces will be realized as one of major factors in the planning and design of offshore dolphins. The direction of the sea berth should be determined with due consideration for the direction of the swell approach because the wave force decreases rapidly as θ_o deviates from $\theta_o = 90^o$. The long period waves should also be prevented from approaching the sea berth.

There remain several problems in the computation of wave forces. They are:

1) The equations on the wave forces have not been confirmed in the experiments though the equations on the reflection and the diffraction by insular breakwaters have been confirmed in the experiments[1].
2) The influence of the clearance between the vessel and the sea bottom on wave forces has not been clarified. The influence is expected to increase as the clearance becomes large.
3) The movement of vessels in mooring is not taken into account. Theory should be developed with experimental verification.
4) The form of the angular distribution or two dimensional wave spectral form should be made clear by the investigation of actual sea waves.

The first two problems are under study in the authors' laboratory and the results will be reported in near future.

CONCLUSION

(1) The theoretical solution of the wave action upon the elliptical cylinder is derived and computation is made for wave forces. The component wave forces in x- and y-direction for the aspect ratio of $b/a = 0.15$ differ depending upon the angle of the wave approach, but the non-dimensional force of F_y has the maximum at about $a/L = 0.4$ irrespective of the angle of wave approach.

(2) The virtual mass coefficients of the elliptical cylinder vary with parameters of b/a, D/L, and α ; they are shown in graphical forms.

(3) The irregular wave forces acting upon the vessel fixed in position have been computed with the approximation of the geometry of a vessel with the elliptical cylinder having the same width-to-length ratio.

(4) Wave forces in the direction of beam decrease rapidly as the angle of wave approach deviates form the beam, but the forces in the longitudinal direction vary a little with the angle of wave approach.

(5) The forces acting upon the offshore dolphins through the vessel are demonstrated to be one of major design factors; the one-third maximum value of thrusts and pulls to a dolphin is estimated as 1,400 tons even for the waves of $H_{1/3} = 1.0m$, $T_{1/3} = 10$ sec, approaching from the beam.

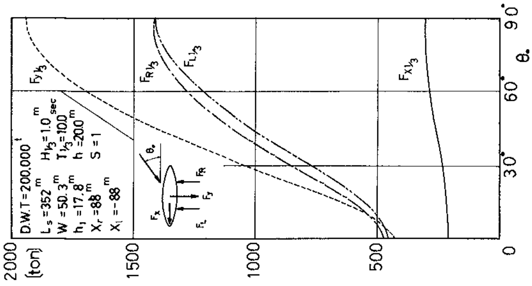

Fig. 8 Variation of one-third maximum forces ($H_{1/3}$ = 1.0m, $T_{1/3}$ = 10 sec)

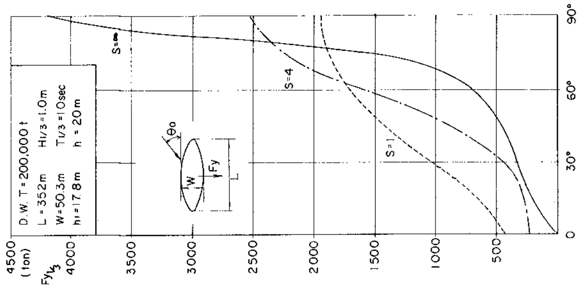

Fig. 9 Variation of $Fy_{1/3}$ for s ($H_{1/3}$ = 1.0m, $T_{1/3}$ = 10 sec)

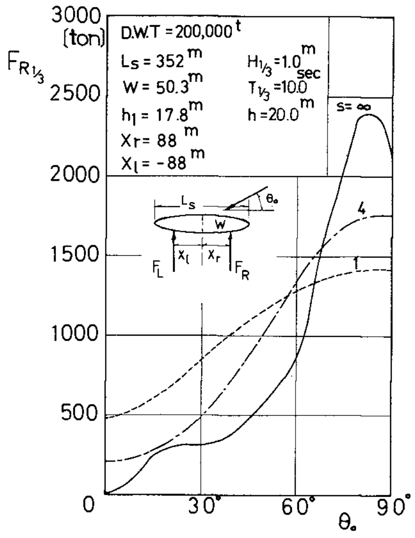

Fig. 10 Variation of $F_{R1/3}$ for s ($H_{1/3}$ = 1.0m, $T_{1/3}$ = 10 sec)

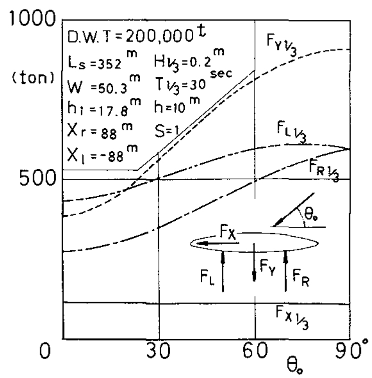

Fig. 11 Variation of one-third maximum forces ($H_{1/3}$ = 0.2m, $T_{1/3}$ = 30 sec)

REFERENCES

1) Goda, Y., Yoshimura, T., and Ito, M. (1971) : Reflection and diffraction of water waves by an insular breakwater, Report of the Port and Harbour Research Institute, Vol. 10, No.2, pp.3 - 52 (in Japanese)

2) Mclachlan, N.W. (1964) : Theory and application of Mathieu functions, Dover Pub. Inc. New York.

3) MacCamy, R.C. and Fuchs, R.A. (1959) : Wave force on piles; diffraction theory, Tech. Mems, No.69, BEB

4) Goda, Y. and Yoshimura, T. (1971) : Wave force computation for structures of large diameter, isolated in the offshore, Report of the Port and Harbour Research Institute, Vol.10, No.4, pp.3 - 52(in Japanese)

5) Neumann, G. (1953) : On the ocean wave spectra and a new method of forecasting wind-generated sea, Tech. Memo., No.43, BEB

6) Bretschneider, C.L. (1959) : Wave variability and wave spectra for wind-generated gravity waves. Tech. Memo., No.118, BEB

7) Pierson, W.T. and Moskovitz, L.(1965) : A proposed spectra form for fully developed wind sea based on the similarity theory of S.A. Kitaigoloskii, Jour. Geophysical Res., Vol.69, No.24, pp.5181 - 5190

8) Refered from Ocean physics III (1971) by Nayata, U., Hikosaka, S. and Miyazaki, M., pp.53 - 87 (in Japanese)

9) Ewing, J.A. (1969) : Some measurement of the directional wave spectrum, Jour. Marine. Res., Vol.27, No.2, pp.163 - 171

10) Longuet-Higgins, M.S. (1952) : On the statistical distribution of the heights of sea waves, Jour. Marine. Res., Vol.XI, No.3, pp.245 - 266

11) Goda, Y., Nagai, K. and Ito, M. (1971) : Wave observation at the Port of Nagoya, third report. Diffraction and statistics of wind waves, Tech. Note of the Port and Harbour Research Institute, No. 120, P.24 (in Japanese)

12) Goda, Y. (1970) : Namerical experiment on wave statistics with spectral simulation, Report of the Port and Harbour Research Institute, Vol. 9, No. 3, pp.3 - 51